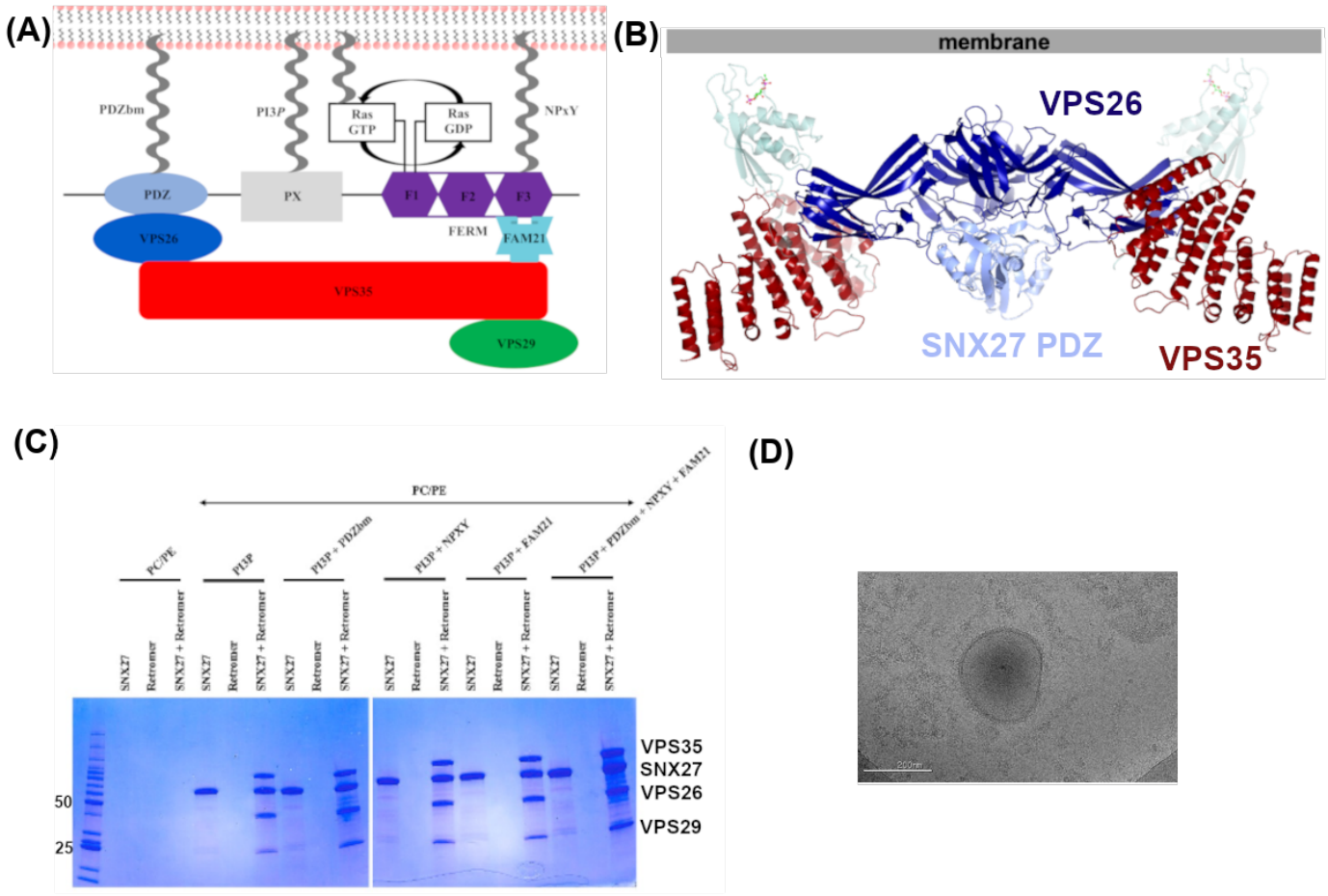

Figure 1. SNX27/retromer reconstitution on membranes. (A) SNX27/retromer domain architecture with binding motifs modelled on a membrane. (B) Model of SNX27 binding to VPS26, in same orientation as (A). This model is based on SNX3/retromer coats (PDB: 7BLO) and SNX27/VPS26 (PDB: 4P2A) structures. The SNX27 PDZ domain is occluded from the membrane by VPS26 dimers, which implies SNX27 could not bind PDZ cargoes in the membrane in this orientation. (C) Liposome pelleting assays reveal conditions for recruiting SNX27/retromer efficiently to PI3*P*-enriched membranes. SNX27 uses its PX domain for membrane recruitment, and retromer requires SNX27 to bind membranes in the presence of PI3*P*. Addition of cargo and regulatory partners substantially enhances SNX27/retromer recruitment (far right). These data suggest optimal conditions for recruiting SNX27/retromer to PI3*P*-enriched liposomes for cryoET studies. (D) Example coated liposome observed in vitreous ice. We observe large liposomes with “fuzzy” protein coats, but we do not see robust tubulation, despite efficient membrane recruitment. Scale bar: 200 nm.

(A) Purification

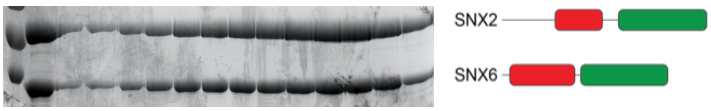

(B) SEC-MALS

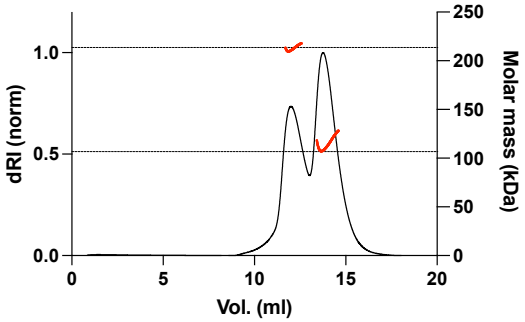

Figure 2. SNX2/SNX6 purification and characterization. (A) Example SDS-PAGE gel of SNX2/SNX6 following purification by affinity chromatography and size exclusion. Domain schematics are shown to right, with PX domains in red and BAR domains in green. (B) SEC MALS data on purified SNX2/SNX6. Data suggest this complex exhibits in a tetramer/dimer equilibrium; the first peak is consistent with a heterotetramer and the second with a heterodimer.

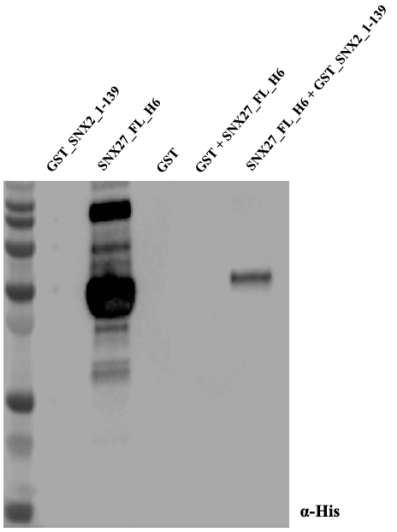

Figure 3. SNX27 directly binds SNX2 N-terminus. Pulldown experiments using purified recombinant proteins indicate the SNX2 N-terminus (GST-tagged residues 1-139) can pulldown full-length SNX27. Western blot against SNX27 His6 tag shown. Both SNX1 and SNX2 harbor conserved motifs in their extended N-termini that can engage SNX27. Calorimetry data with peptides (not shown) indicate micromolar Kds.

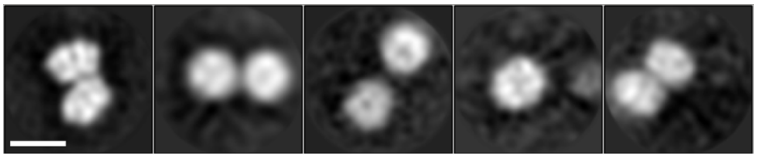

Figure 4. 2D classification of β'-COP (1-604)/Glo3 (230-300) complex. Representative classes from 5,000 manually picked particles (1.096 Å/pixel bin) from recent NCCAT data collection. We currently have 3.4 million particles after auto-picking. These data suggest we can pursue single particle structures of β'-COP with a variety of binding partners. Scale bar: 50 Å.

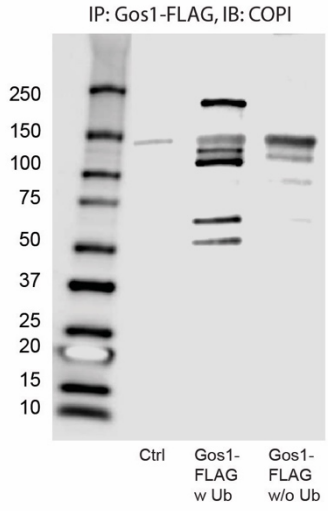

Figure 5. Gos1 immunoprecipitates COPI under ubiquitination conditions. The FLAG-tagged yeast SNARE, Gos1, efficiently pulls down COPI coat subunits when ubiquitin (Ub) conditions are preserved in yeast cells. The interaction is lost in the presence of enzymes that remove ubiquitin linkages. Immunoblot using COPI coat antisera (Barlowe lab, Dartmouth). These preliminary data suggest a strategy for purifying COPI coats directly from yeast cells to be used in reconstitution approaches.